Journal of Macromolecular Science, Part A
Publication details, including instructions for authors and subscription information:
http://www.informaworld.com/smpp/title~content=t713597274

Poly(acrylamide-co-2-acrylamido-2-methyl-1-propanesulfonic Acid) Nanogels made by Inverse Microemulsion Polymerization

Pallavi Bhardwaj[a]; Vaishali Singh[a]; Saroj Aggarwal[a]; Uttam Kumar Mandal[ab]
[a] University School of Basic and Applied Sciences, Guru Gobind Singh Indraprastha University, Delhi, India [b] University School of Chemical Technology, Guru Gobind Singh Indraprastha University, Delhi, India

To cite this Article Bhardwaj, Pallavi , Singh, Vaishali , Aggarwal, Saroj and Mandal, Uttam Kumar(2009) 'Poly(acrylamide-co-2-acrylamido-2-methyl-1-propanesulfonic Acid) Nanogels made by Inverse Microemulsion Polymerization', Journal of Macromolecular Science, Part A, 46: 11, 1083 — 1094
To link to this Article: DOI: 10.1080/10601320903256497
URL: http://dx.doi.org/10.1080/10601320903256497

Journal of Macromolecular Science®, Part A: Pure and Applied Chemistry (2009) **46**, 1083–1094

ISSN: 1060-1325 print / 1520-5738 online
DOI: 10.1080/10601320903256497

Taylor & Francis
Taylor & Francis Group

Poly(acrylamide-co-2-acrylamido-2-methyl-1-propanesulfonic Acid) Nanogels made by Inverse Microemulsion Polymerization

PALLAVI BHARDWAJ, VAISHALI SINGH, SAROJ AGGARWAL and UTTAM KUMAR MANDAL*

University School of Basic and Applied Sciences, Guru Gobind Singh Indraprastha University, Kashmere Gate, Delhi-110 403, India
**University School of Chemical Technology, Guru Gobind Singh Indraprastha University, Kashmere Gate, Delhi-110 403, India*

Received March 2009, Accepted May 2009

Poly(acrylamide-co-2-acrylamido-2-methyl-1-propanesulfonic acid) poly(AM-co-AMPSA) nanogels were prepared through inverse microemulsion polymerization with low AMPSA/AM weight ratio in the feed (up to 0.3357) to control particle size and pH sensitivity. An aqueous solution of AM and AMPSA was used as the dispersed phase for microemulsion with sodium bis(2-ethylhexyl) sulfosuccinate (AOT)/Toluene solution as the dispersion medium. The polymerization was carried out at 50°C in the presence of 2,2-azobisisobutyronitrile (AIBN) and N,N′-methylenebisacrylamide (NMBA) as an initiator and a crosslinker, respectively. Fourier transform infra red spectrophotometer (FTIR) and ^{1}H-nuclear magnetic resonance spectroscopy (^{1}H-NMR) studies confirm the occurrence of copolymerization between the two monomers. The hydrodynamic diameter of synthesized poly(AM-co-AMPSA) nanogels is found to be in the range of 63–125nm as measured by dynamic light scattering (DLS). The equilibrium swelling and the effect of pH on particle size of copolymer nanogel are found to depend on the copolymer composition. The polymer chain composition, thermal properties and morphology of nanogels were measured by elemental analysis, thermogravimetric analyzer (TGA) and differential scanning calorimeter (DSC), and scanning electron microscope (SEM), respectively.

Keywords: Inverse microemulsion, nanogels, acrylamide, 2-acrylamido-2-methyl-1-propanesulfonic acid, pH

1 Introduction

The research field in the domain of nanoscience and nanotechnology has attracted much attention in the recent years. The great interest lies in the fact that selective reactivity of macromolecules controlled over nanoscale dimensions is providing the means to prepare unique nanomaterials (nanogels/microgels) for fundamental and applied studies in nanoscience and nanotechnology. Such knowledge can be applied for designing of sophisticated polymeric nanogels for advanced applications like in targeted radiopharmaceuticals (1), field emissive displays and cathode ray tube (2) etc. Nanogels are internally crosslinked structures and are intermediate between branched and macroscopically crosslinked polymers. Dimensionally nanogels can be considered as colloidal particles with average diameter in the range of ten to few hundred of nanometre.

Poly(acrylamide) (PAM) and poly(N-isopropylacrylamide) (PNIPAM) hydrogels are attractive 'smart' materials that have important applications in medicine and bioengineering because of their thermo-reversibility. However, these hydrogels recently have attracted increasing attention because of the fast dynamics in swelling or collapsing processes. The swelling or collapsing of temperature response latex particles dispersed in water is an intraparticle phenomenon, but as is well-known, interparticle aggregation also takes place during the collapse transition. Incorporation of ionizable monomers in a PAM matrix demonstrates higher swelling and deswelling behavior of hydrogels. Therefore, in the recent years, several attempts have been made to broaden the applicability of environmental stimuli-responsive 'smart' polymeric gel materials by incorporating functional groups within the microgel matrix (3–5). These materials can be obtained for example by copolymerization of AM/NIPAM with an ionic monomer (6–9). The behavior of these "smart" polymers governed by combination of electrostatic and hydrophobic interactions, leads to unique properties which can be capitalized upon in a

*Address correspondence to: Uttam Kumar Mandal, University School of Chemical Technology, Guru Gobind Singh Indraprastha University, Kashmere Gate, Delhi-110 403, India. Tel.: 91-011-23900247; Fax: 91-11 -23865941; E-mail: uttammandal@rediffmail.com
Pallavi Bhardwaj, Tel.: 91-011-23900281; E-mail: pallavibhardwaj2009@gmail.com Vaishali Singh, Tel.: 91-011-23900281;
E-mail: dr_vaishali_singh@yahoo.co.in
Saroj Aggarwal, Tel.: 91-011-23900282;
E-mail: s_kka@yahoo.com

number of applications including the preparation of magnetic functionalized nanogels (10), as templates for nanoparticle synthesis (11), fabrication of photonic crystals (12), microlens arrays (13), specific targeting of cancer cells and drug delivery systems (14–16).

For many applications, nanogels with large water absorption capacity and favorable thermo-mechanical stability in the swollen state are required (17, 18). These properties can be usually obtained by incorporation of functional groups in the polymer chains. Extensive work has been reported for the synthesis of functionalized nanogels based on copolymerization of AM/NIPAM with carboxylic/sulfonic acid containing monomer by plasma-initiated, solution or dispersion polymerization (19–21). The recent progress in the field is towards the synthesis of copolymer microgels based on sulfonic acid-acrylamide by microemulsion polymerization (22–24). It has also been reported that polymerization reaction carried out in nanostuctured media like micelles or microemulsions allow the synthesis of smart polymeric nanogels with controlled architecture and well defined characteristics (25–27). The small particle size and narrow size distribution obtained from inverse microemulsion polymerization method make this method attractive for the preparation of nanogels.

Although most of these reports have highlighted the effect of functional comonomers on the swelling and deswelling properties of hydrogels at neutral medium or higher pH (28–30), very little literature is available on particle size distribution, thermal stability and phase morphology of copolymer nanogels made by inverse microemulsion polymerization. The present purpose of our study is to investigate the effect of copolymer composition on size, equilibrium swelling and pH sensitivity of copolymer nanogels. We have synthesized low AMPSA containing co-polymeric nanogels through water-in-oil (W/O) microemulsion polymerization and the size, polydispersity, presence of functional groups, thermal stability and morphology of copolymers have been investigated by DLS, FTIR, ^{1}H-NMR, elemental analysis, TGA, DSC, and SEM.

The monomers which have been chosen for this study are AM and AMPSA as neutral and acidic monomers in nature respectively. AMPSA has strongly ionizable sulfonate group (31) and is known for its hydrolytic stability, high tolerance towards divalent cations (32). The presence of $-SO_3^-$ group in AMPSA offers high stability in solution due to stronger hydrogen bonding capability and polyelectrolyte behavior in aqueous solutions (33). Moreover $-SO_3^-$ group imparts greater hydrophilic character and causes more swelling of nanogels in water.

2 Experimental

2.1 Materials

AM, AMPSA, AOT were purchased from Aldrich and used directly without further purification. Extrapure AIBN and NMBA were purchased from a local market and used as received. AR grade toluene received from SRL (India) was distilled prior to use. Double distilled water drawn from a millipore purification system was used.

Table 1. The composition of W/O microemulsion system for Poly(AM-co-AMPSA) nanogel synthesis

Samples composition (gm)	CP_0	CP_5	CP_{10}	CP_{15}	CP_{25}
Toluene	59.64	59.64	59.64	59.64	59.64
AOT	23.81	23.81	23.81	23.81	23.81
Water	12.73	12.73	12.73	12.73	12.73
AM	3.82	3.63	3.44	3.25	2.86
AMPSA	0	0.19	0.38	0.57	0.96
AIBN	0.0382	0.0382	0.0382	0.0382	0.0382
NMBA	0.0382	0.0382	0.0382	0.0382	0.0382
Time for complete reaction (min.)	60	45	40	25	25

2.2 Preparation of Poly(AM-co-AMPSA) Copolymer Nanogels

The aqueous phase of microemulsion system was obtained by dissolving the desired amount of AM and AMPSA in 12.73 ml of water (Table 1). In the W/O microemulsion process, 23.81gm AOT was dissolved in 59.64 gm of toluene in a 250 ml conical flask. Now, the above prepared aqueous solution of monomers was added dropwise to a surfactant solution to form W/O microemulsion. This microemulsion was transferred to 250 ml, two-neck round bottom flask fitted with a condenser and a nitrogen gas inlet. It was stirred on a magnetic stirrer at 1000 rpm for 6 h. AIBN and NMBA (each 1 wt% of monomers) were added to initiate the polymerization and for crosslinking. The microemulsion was then purged with nitrogen gas for 30 min. The polymerization mixture was then heated in a constant temperature water bath at 50°C for a different time period to attain complete conversion (Table 1). After polymerization, the mixture was cooled to room temperature and acetone was added to precipitate the polymerized product. The precipitates were separated and washed several times through centrifugation first with CH_3OH to remove residual monomer and then with toluene to remove AOT. The precipitates were then dried in vacuum oven at 50°C. PAM nanogels were also prepared in similar way without AMPSA.

2.3 Characterization of Nanogels

A Malvern zetasizer nano series (Malvern instruments Ltd., U. K.) was used to measure the size of the reverse micelle of microemulsion droplet and poly(AM-co-AMPSA) nanogels. It measures the scattering information close to 180° (backscatter detection) using patented NIBS^{TM} (Non Invasive Back Scattering) technology to increase detection sensitivity and reduce multiple scattering (minimum at

180° hence, higher concentration can be measured). DLS measurements were performed at 25°C in a square glass cuvette with round aperture at a fixed angle of 173°. The values of dispersant refractive index and viscosity of toluene were taken 1.491, 0.5500 cP, respectively.

The FTIR spectra were collected on a Shimadzu Japan FTIR-8700 Fourier transform infrared spectrophotometer in the range of 4400–400 cm^{-1}. Samples of isolated particles of prepared nanogels were mixed with KBr, homogenized and converted into pellets under a pressure of 8 ton and the spectra (absorbance with wave number) were taken thereafter.

^{1}H-NMR spectra of poly(AM-co-AMPSA) nanogels were recorded using a Bruker DRX400 MHz spectrometer. Tetramethylsilane (TMS) was used as the reference and deuterated water (D_2O) as the solvent.

The percentage of elements in the copolymer was determined by a Vario EL III CHNS analyzer, Germany.

The TGA was performed using a Perkin-Elmer TGA7 thermobalance. The dried samples in a nitrogen atmosphere were analyzed in the temperature range of 50°C to 760°C at the scanning rate of 20°C/min.

DSC Q10, TA Instruments, USA was used to study the glass transition temperature of poly(AM-co-AMPSA) nanogels. About 2 mg of the sample was sealed in an aluminum DSC pan and heated from 50°C to 350°C at a heating rate of 10°C/min under nitrogen purge flow (50 ml/min).

The surface morphology of the dried poly(AM-co-AMPSA) nanogels was studied using SEM (LEO 435 VP) operated at 15kV. Coating was carried out under reduced pressure in an inert argon gas atmosphere (Agar Sputter Coater P7340).

3 Results and Discussion

DLS is a well established technique for measuring micelle size in the nm range. Micelle size of prepared microemulsions is found below 10 nm. In the present investigation, we have reported a low dose of AMPSA monomer in the microemulsion system, as during microemulsion preparation it was found that the high dose of AMPSA makes the system unstable. The polymerization (Fig. 1 schematic representation of copolymer formation) was monitored by DLS to measure the influence of acidic monomer on nanogel size, equilibrium swelling and pH sensitivity. Table 2 summarizes the size of poly(AM-co-AMPSA) nanogels as synthesized in the microemulsion, as well as in the aqueous medium with different copolymer composition. As compared to the size of monomer laden micelles in microemulsion environment, the size of nanogel dispersed in toluene is found to be larger as reported in the literature (29). It is also evident that the presence of acidic monomer in poly(AM-co-AMPSA) nanogels shows a higher size of particle than a pure PAM particle. This may be due to higher swelling of copolymer in the microreactor in toluene continuous phase with limited water droplets as incorporation of AMPSA increases the hydrophilicity of the particles leading to a better solvation.

Figure 2 indicates that the sharp peak of pure PAM has been changed to broader peak in CP_{10}. Moreover, both primary and secondary particles are obtained for CP_{15} and

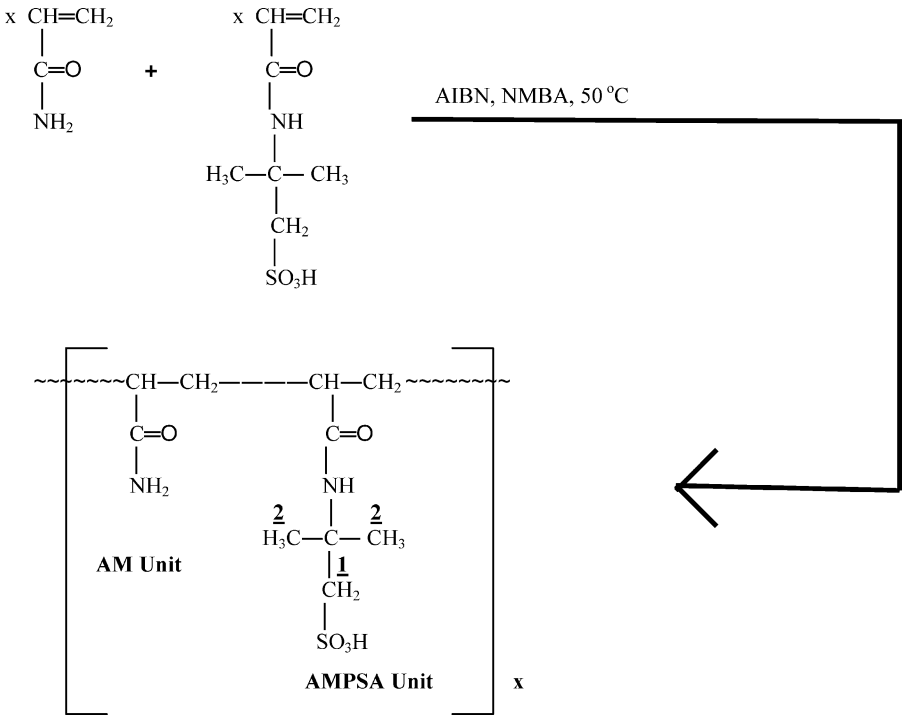

Fig. 1. Schematic representation of copolymer formation.

Table 2. Particle Size of Poly(Am-co-Ampsa) Nanogels in Microemulsions and Aqueous Medium

Samples	*Polymerized microemulsion D_H (nm)*	*PDI in microemulsion*	*pH of nanogel*	*Size of nanogel in aqueous medium D_H (nm)*	*PDI in aqueous medium*
CP_0	63	0.243	6.59	80	0.351
CP_5	72	0.284	6.50	103	0.375
CP_{10}	96	0.392	5.77	150	0.419
CP_{15}	105	0.314	4.88	185	0.438
CP_{25}	125	0.709	4.40	237	0.880

CP_{25} with high values of polydispersity index (Table 2). It is also observed that during polymerization the presence of high dose of AMPSA imparts a certain degree of catalytic behavior towards microemulsion polymerization. This catalytic activity promotes rapid reaction and simultaneously increases the formation of both primary and secondary particles with increasing AMPSA.

The pH for each sample of poly(AM-co-AMPSA) nanogels and pure PAM dispersed in deionized water were measured and is found lowest for CP_{25} sample, i.e., 4.4 which indicates the increase in AMPSA content in the copolymer chains with increasing feed composition (Table 2). The hydrodynamic diameter (number average) of hydrogels at equilibrium swelling in deionized water measured by DLS is found in the range of 80–237 nm. Using the size of nanogels in polymerized microemulsion (volume in relaxed state) and deionized water (volume in fully swollen state), the apparent swelling ratio is calculated using the following formula (29),

$$\text{Apparent Swelling Ratio} = \frac{V_{\text{swollen}}}{V_{\text{relaxed}}} = \left(\frac{D_{\text{h aqueous solution}}}{D_{\text{h polymerized microemulsion}}}\right)^3$$

Figure 3 shows that swelling of poly (AM-co-AMPSA) nanogels in aqueous medium increases with increasing AMPSA/AM feed ratio. The increase in size at equilibrium

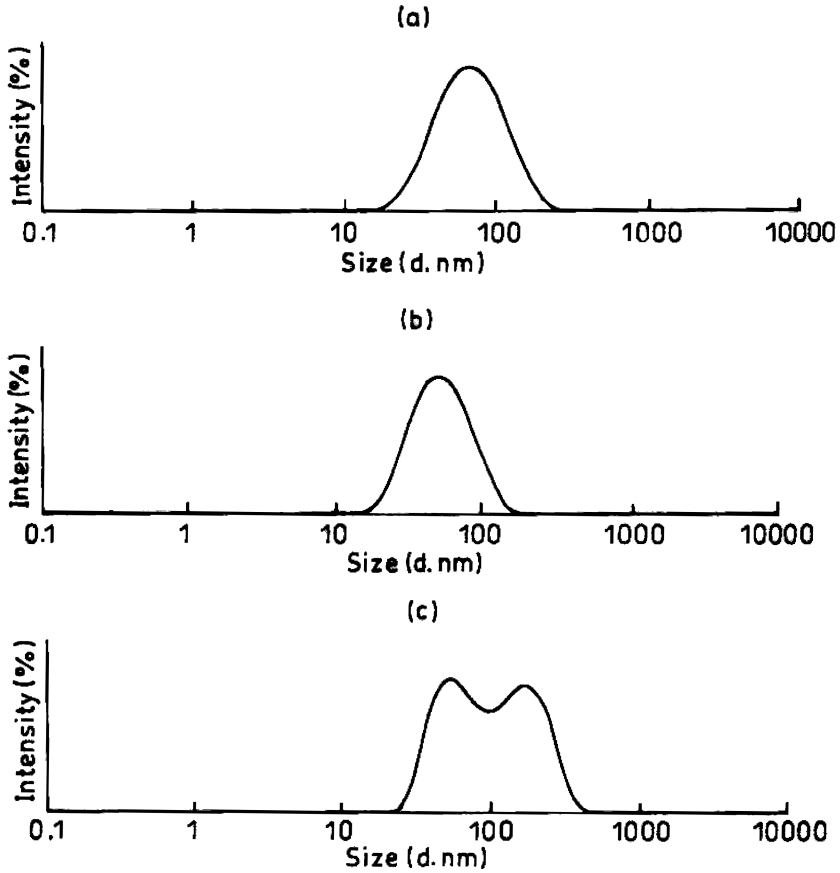

Fig. 2. Size distribution curves of nanogels with variation of AMPSA concentration in monomer phase: (a) CP_0, (b) CP_5, and (c) CP_{10}.

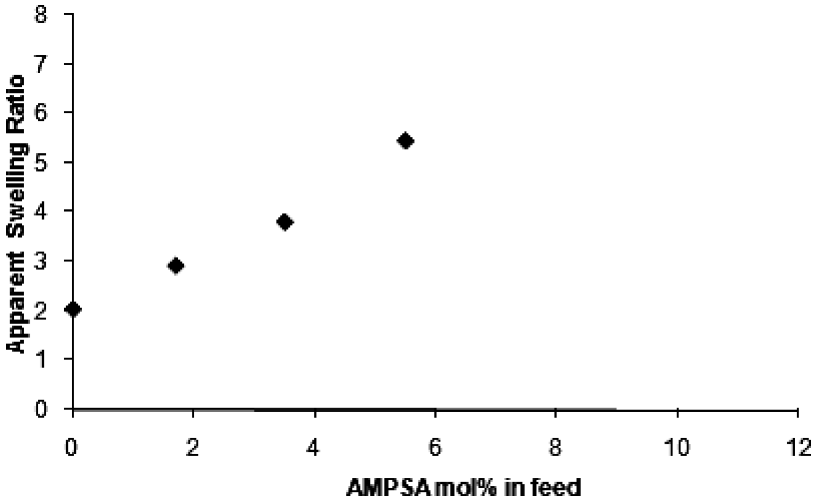

Fig. 3. Apparent Swelling Ratio of poly(AM-co-AMPSA) nanogels.

swelling is due to linkage of AM with highly charged AMPSA which introduces a high degree of hydrophilic character in the copolymer nanogel. The higher value of apparent swelling ratio for CP_{15} is attributed to higher dose of AMPSA monomer causing excessive swelling due to high solvation of copolymer nanogel. The apparent swelling ratio of CP_{25} (with 0.3357 AMPSA/AM weight ratio in feed) is not reported due to multimodal distribution of the particles as synthesized in the microemulsion. As water is a good solvent for protonation of sulfonic groups in poly(AM-co-AMPSA) nanogels, it promotes the solvation of the particles and expands the size of nanogels. Also osmotic pressure of the counterions and electrostatic repulsions between charged sulfonic groups results in more swelling of the nanogels and thus increasing the size in the aqueous phase. Presence of sulfonic group influences the swelling through electrical repulsions between the particles and osmotic pressure (arising from mobile counterions). Thus, the presence of AMPSA increases the affinity of copolymer nanogels towards water, making them extremely hydrophilic to absorb more water for high degree of swelling.

Figure 4 shows the hydrodynamic diameter of different copolymeric nanogels as a function of pH. The dimensions of the copolymeric nanogels is slightly affected by pH of the aqueous phase at higher dose of sulfonic content. Although measurements of the swelling behavior of acid functionalized copolymer nanogels are problematic due to ionic effect of added salt but the addition of small amount (in microlitre) of dilute HCl (0.004N) and NaOH (0.005N) have only small/negligible ionic strength effect (34). This procedure also produces a minor imprecision with respect to the pH value. The figure also indicates that the swelling increases gradually with increase of the sulfonic content in the nanogel structure at specific pH as repulsion forces within the nanogel particle becomes stronger at higher concentration of charged sulfonic groups. The slight decrease in hydrodynamic diameter at higher pH is may be due to the increase of the ionic strength by excess of NaOH and hence, screening the electrostatic repulsion within the nanogel particles (35–36). Here only a small ionic strength has been considered. However, these effects are smaller than the changes of ionic strength which would be caused by the use of a buffer or NaCl solution. It is also reported that the size of the nanogels remains unaffected in the overall range of pH due to the presence of ionizable sulfonic groups in polymer chains (37,38).

The FTIR spectra of the dried poly(AM-co-AMPSA) nanogels in the absorbance mode are shown in Figure 5. The N-H stretching of amide group in AM, AMPSA and overlapping O—H stretching of sulfonic acid group in AMPSA is observed in the region 3200–3500 cm^{-1} (39). The strong absorption band in the region 1666–1670 cm^{-1} can be attributed to the C—O stretching of CO in both AM and AMPSA. The strong peak at 1614 cm^{-1} corresponds to N-H bending of NH_2 (δ) and amide II band in AM (40). Secondary amide II band of AMPSA unit is in the range of 1539–1552 cm^{-1}. The sharp peak of sulfonic ($-SO_3H$) acid

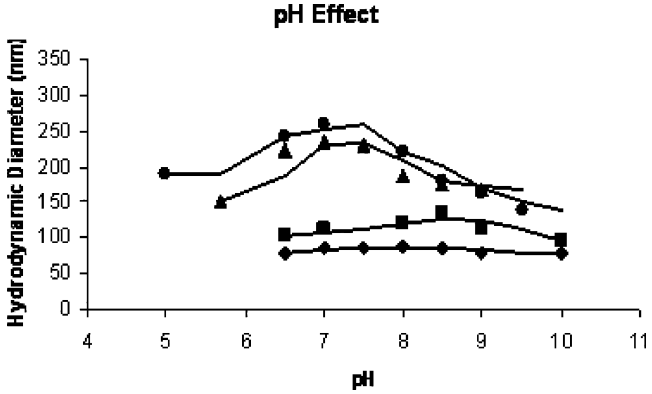

Fig. 4. Effect of pH on hydrodynamic diameter of copolymeric nanogels: ♦ CP_0, ■ CP_5, ▲ CP_{10}, and ● CP_{15}.

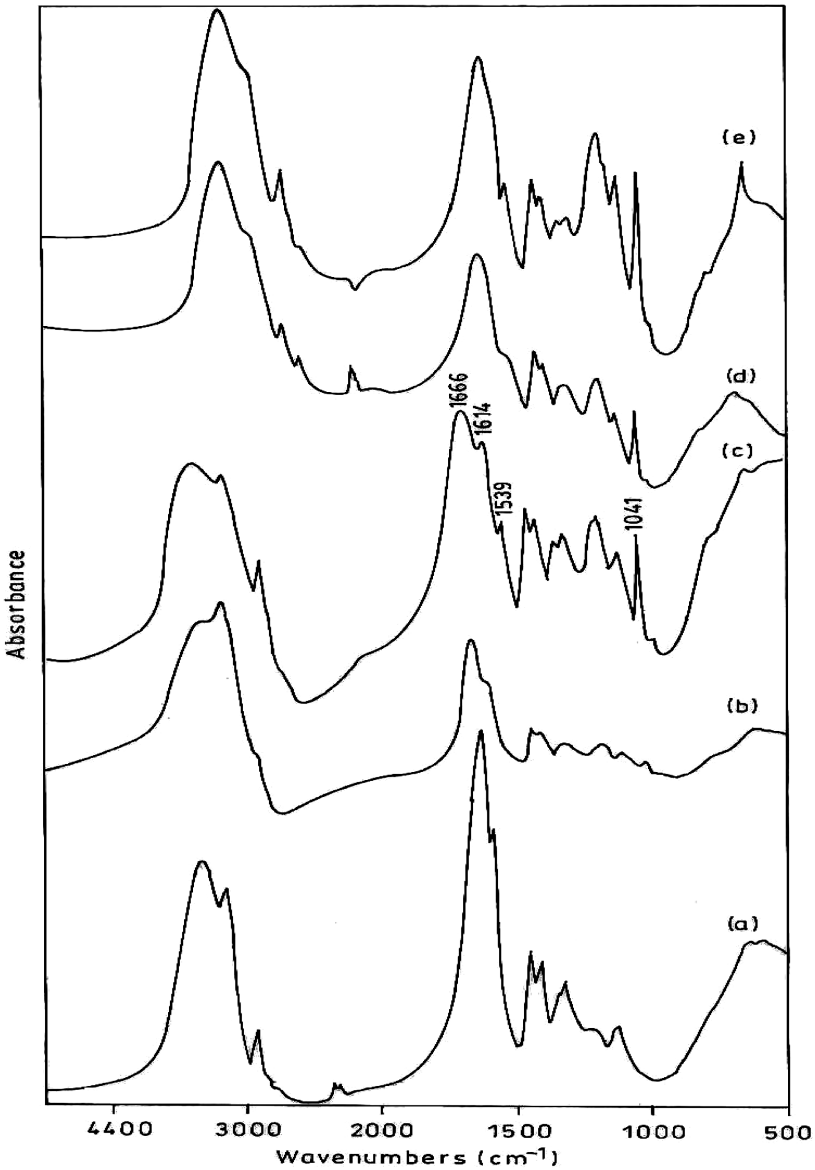

Fig. 5. The FTIR spectra (range 4400–400 cm^{-1}) of poly(AM-co-AMPSA) nanogels: (a) CP_0, (b) CP_5, (c) CP_{10}, (d) CP_{15}, and (e) CP_{25}.

group (41) is in the 1041–1043 cm^{-1} region. The asymmetric band of SO_2 is observed in the range of 1184–1190 cm^{-1}. Table 3 gives the main characteristic peak assignment of the FTIR spectra. The absence of olefinic band at 1620–1635 cm^{-1} confirms the product contained poly(AM-co-AMPSA) nanogels and excluded the presence of monomer. When the weight ratio of AMPSA/AM is minimum (CP_5 sample), the characteristic peak of sulfonic acid group is quite weak. However, the spectrum result clearly indicate that by increasing the weight ratio of AMPSA/AM in the nanogel composition -SO_3H peak intensity increases.

The secondary amide group is linked with H-bonding. This bonding behavior is formulated on the basis of the fact that the presence of peak at 1553 cm^{-1} in CP_{15} has changed to 1539 cm^{-1} in CP_{25} with certain degree of broadness in peak. The strong H-bonding results in a decrease of absorbance. The results demonstrate that there are a large amount of H-bonds between $-SO_3H$ and $-CONH_2$ of poly(AM-co-AMPSA). The concentration of AMPSA monomer determines the macromolecular chain composition in nanogel. Further, this chain composition is the basis for determination of H-bonds formed in nanoreactors.

The ^{1}H-NMR spectrum of poly(AM-co-AMPSA) (CP_{10} sample) in the non crosslinked state is shown in Figure 6. The NMR spectrum of the nanogel has the characteristic peaks of the polymeric units. A singlet in the NMR spectrum at 1.30 ppm shows that two methyl groups, i.e.

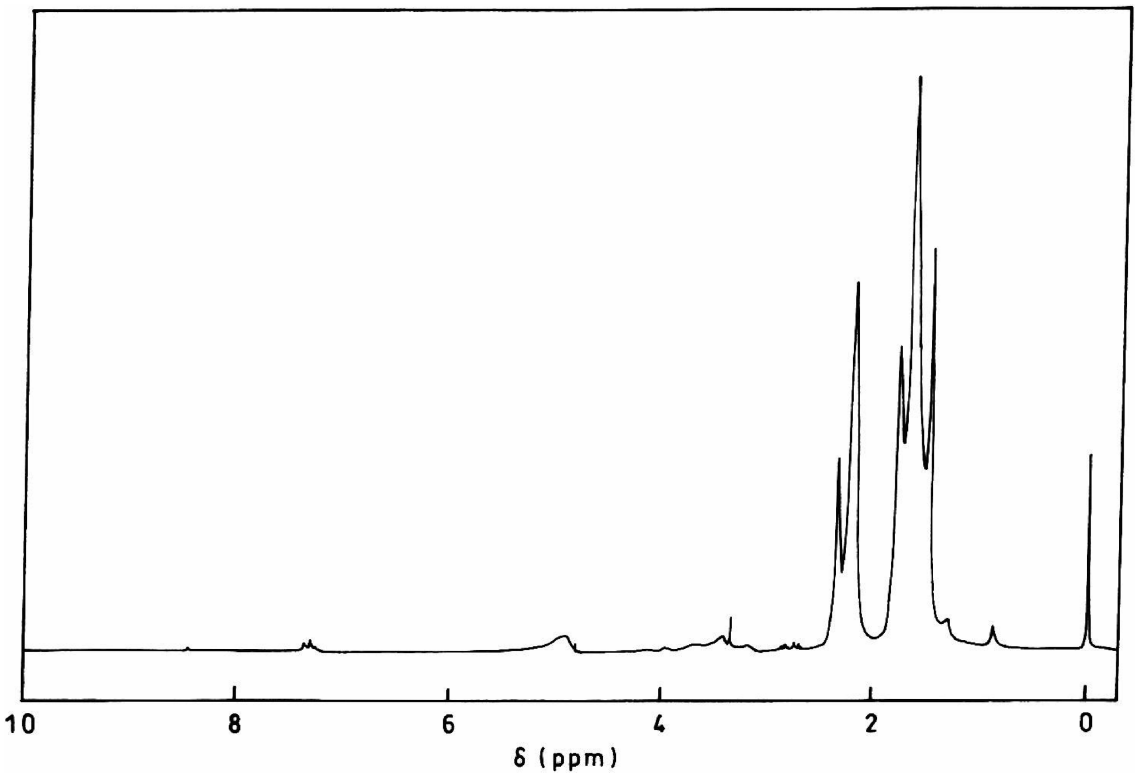

Fig. 6. ^{1}H-NMR spectrum of poly(AM-co-AMPSA) (CP_{10} sample).

$(CH_3)_2$—C— in AMPSA are in similar chemical environment (42). The hydrogen of the CH_2 group bonded to sulfonic acid group gives a signal at 3.2 ppm (33). The protons **1** and **2** in Figure 1 being shielded, the field felt by such protons is less and hence, resonance occurs upfield. In general, the δ value shows the order Methyl < Methylene < Methine. The peak for the proton of the $-SO_3H$ is not detected in the spectrum, indicating that this hydrogen is in permutation with D_2O (41). The peak for deuterated water (D_2O) occurs at 4.85 ppm (42). Table 4 gives chemical shift (ppm) and peak assignment of NMR spectrum.

Elemental analysis of the copolymer nanogels is used to estimate their chemical composition. Table 5 shows chemical composition data of poly(AM-co-AMPSA) nanogels. The fraction of AMPSA in the copolymer nanogels (43), f(AMPSA), is calculated from the following equation (33),

$$\text{f (AMPSA)} = \frac{14.0\ \text{S\%}}{32.1\ \text{N\%}}$$

Where S% and N% are the weight percentage of S and N obtained from elemental analysis. The results indicate that the copolymerization of AM and AMPSA represent a unique condition in inverse microemulsion, since the reactivity ratio of these comonomers is greater than one in solution and emulsion polymerization (33), although these ratios are quite different (less than one) when copolymerization is carried out in inverse microemulsion (43). Intrinsic reactivity of the comonomers in inverted micelles is thus modified for reasons not yet clear, possibly due to specific

Table 3. Peak Assignment of Poly(Am) and poly(AM-co-AMPSA) Nanogels

Peak position (cm^{-1})	*Assignment*
3200–3500	N—H stretching of NH_2 (ν), OH stretching of -SO_3H acid group
1666–1670	C—O stretching of CO in AM, AMPSA
1614	N—H bending of NH_2 (δ), amide II band of AM
1539–1552	Secondary amide II band of AMPSA
1041–1043	S—O_3H acid group
1184–1190	asymmetric band of SO_2

Table 4. Chemical shift (ppm) and peak assignment for poly(AM-co-AMPSA) Nanogels (CP_{10})

δ in ppm	*Interpretation*
1.30	CH_3 in side chain $(CH_3)_2$-C- group of AMPSA
1.49	—CH_2
3.2	—CH_2-SO_3^- (AMPSA)
2.22	—CH—
4.8–4.9	D_2O

Table 5. Elemental analysis results of poly(AM-co-AMPSA) Nanogel

Samples	*Mole fraction of AMPSA monomer in feed*	*S%*	*N%*	*AMPSA in copolymer Nanogel (mol%)*
CP_5	0.017	1.496	14.45	4.51
CP_{10}	0.035	1.936	18.15	4.65
CP_{15}	0.055	2.199	13.51	7.09
CP_{25}	0.102	4.528	11.72	16.85

interactions with the microenvironment. Reaction between the comonomers also seems promoted due to their preferential concentration in the aqueous domain of the microemulsion.

The TGA curves of poly(AM-co-AMPSA) nanogels with different weight ratio of the two monomers are shown in Figure 7. Aggour (44) reported the thermal stability of PAM, PAMPSA and poly(AM-co-AMPSA) using thermogravimetry. PAM and PAMPSA showed appreciable degradation at about 245°C and 182°C, respectively, and a second stage decomposition at about 300°C. He also concluded that the thermal degradation of poly(AM-co-AMPSA) copolymers occurs in three different stages: decomposition of amide groups, degradation of sulfonic groups, and breakdown of the polymer backbone. The TGA curve of PAM nanogels show four stages of weight loss with temperature which has also been reported in our previous work (45). As is evident from Figure 7, TGA curves for all nanogels have characteristic four stages decomposition regions. The first stage weight loss from 60°C–210°C is about 13–22% associated with dehydration of the samples and thermal

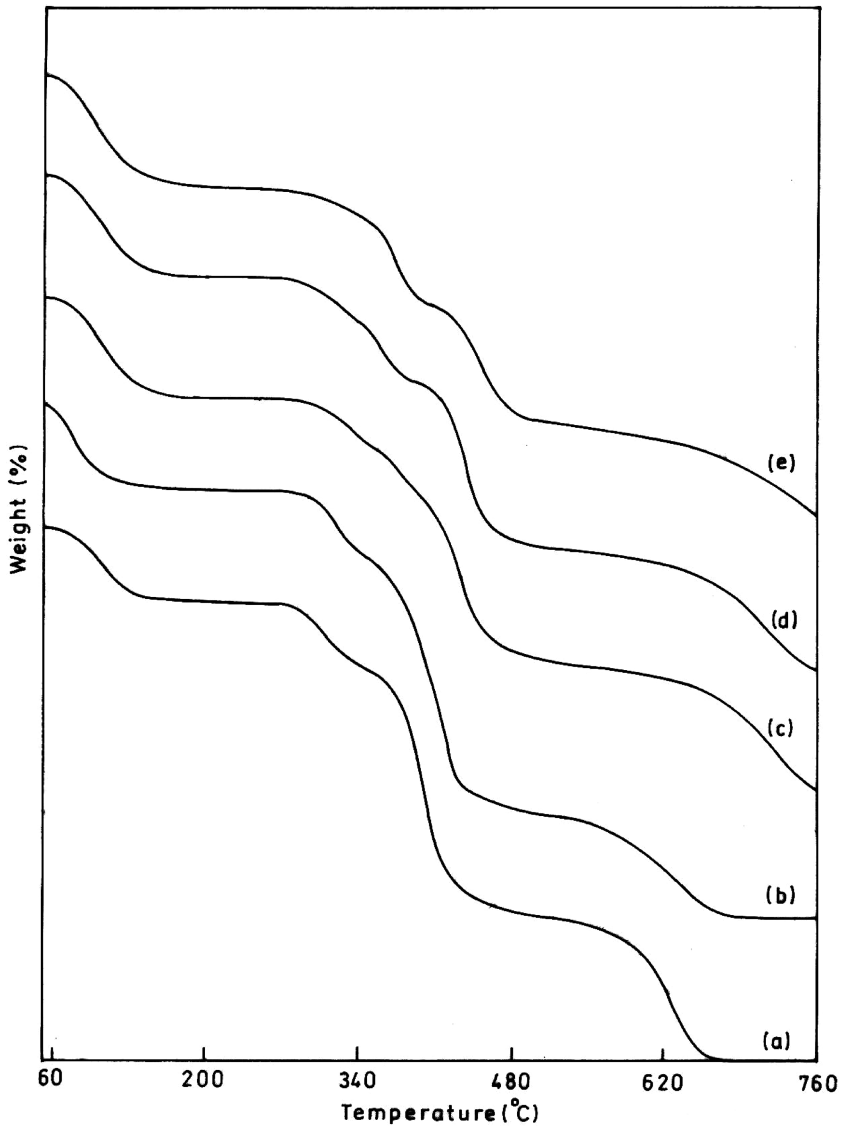

Fig. 7. TGA curves for the nanogels heated to 760°C: (a) CP_0, (b) CP_5, (c) CP_{10}, (d) CP_{15}, and (e) CP_{25}.

degradation occurs in this temperature range causing irreversible chemical changes. The second region is from 220°C–400°C, however, the second stage of degradation reported in literature is about 300°C (44) which may be related to possible degradation of sulfonic groups.

In the second region for all four samples, the sharp degradation temperature is observed and it is maximum for CP_{25}, the higher the ionic group content, and the broader the temperature interval for decomposition of the sulfonic acid group. Here, the weight loss is about 13–23%. The third stage weight loss from 400°C–500°C is about 50%, 34%, 33%, 27% from low towards high content of AMPSA. In this region, the main chain degradation reaction and breakdown of the polymer backbone occurs. Moreover random bond scission of the main polymeric backbone dominates the reaction (46). Last stage decomposition occurs at 540°C–780°C. The TG measurement also reveals that the residue after degradation (1.5%, 4.6%, 4.8%, and 12.4%) increases with increasing AMPSA/AM weight ratio. Copolymers show a very high thermal stability, which increases with increasing acidic AMPSA unit content in the copolymers. The increasing thermal stability at higher temperature may be due to the presence of sulfonic groups in side chain, which form cross-links. Also, it is well known that H-bonds as a variety of intermolecular interaction, exert essential influence on chemical structure of polymer formation (47). Due to the formation of H-bonds, physical, physico-chemical, spectral and thermal properties of co-polymers/polymers can be changed essentially.

Figure 8 shows the heating DSC curves obtained for poly(AM-co-AMPSA) nanogels. From these thermograms, the glass transition temperature (T_g), the decomposition temperature (T_d), and the decomposition enthalpy (ΔH_d) have been calculated. The transition temperature (T_g) and heat flow corresponding to decomposition zones are reported in Table 6. First transition peak occurs in the range

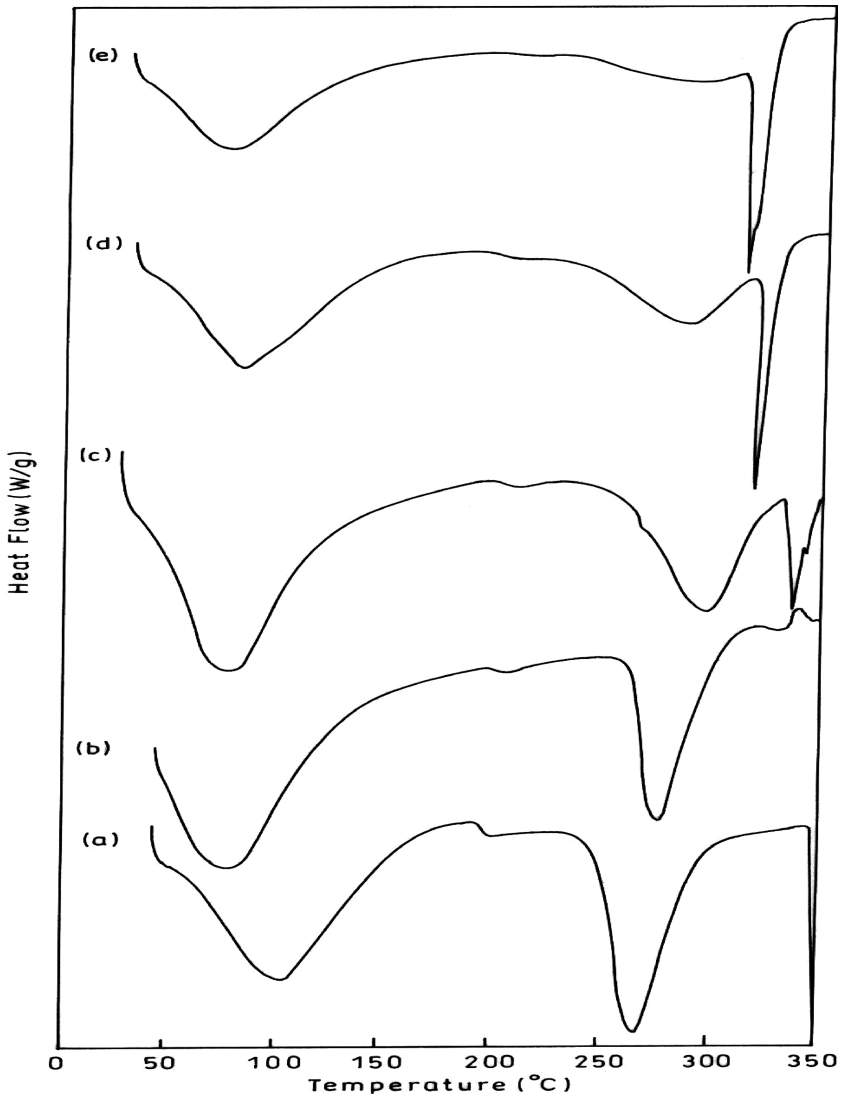

Fig. 8. DSC curves for the nanogels heated to 350°C: (a) CP_0, (b) CP_5, (c) CP_{10}, (d) CP_{15}, and (e) CP_{25}.

Table 6. Thermal parameters obtained by DSC

Samples	T_g (°C)	T_{d1} (°C)	ΔH_{d1} (j/g)	T_{d2} (°C)	ΔH_{d2} (j/g)
CP_0	191.95	266	228.9	—	—
CP_5	194.49	273	147.6	316	5.372
CP_{10}	196.02	297	150.6	336	34.58
CP_{15}	196.63	288	135.1	321	72.80
CP_{25}	197.00	—	45.08	317	141.80

of 74°C–83°C which is probably due to loss of water content in the materials. The second endotherm peaks are in the range of 273°C–297°C and attributed to amide group degradation and the cleavage of weak crosslinks. The gradual increase of broadness of this endotherm and decrease in the sharpness of peaks are observed with increasing AMPSA content in the copolymer. The third decomposition peaks are in the range of 317°C–336°C. This region is probably due to sulfonic acid group degradation of AMPSA backbone (48). The decrease of decomposition temperature in CP_{15} and CP_{25} is attributed to high% of AMPSA which may increase the free content of sulfonic

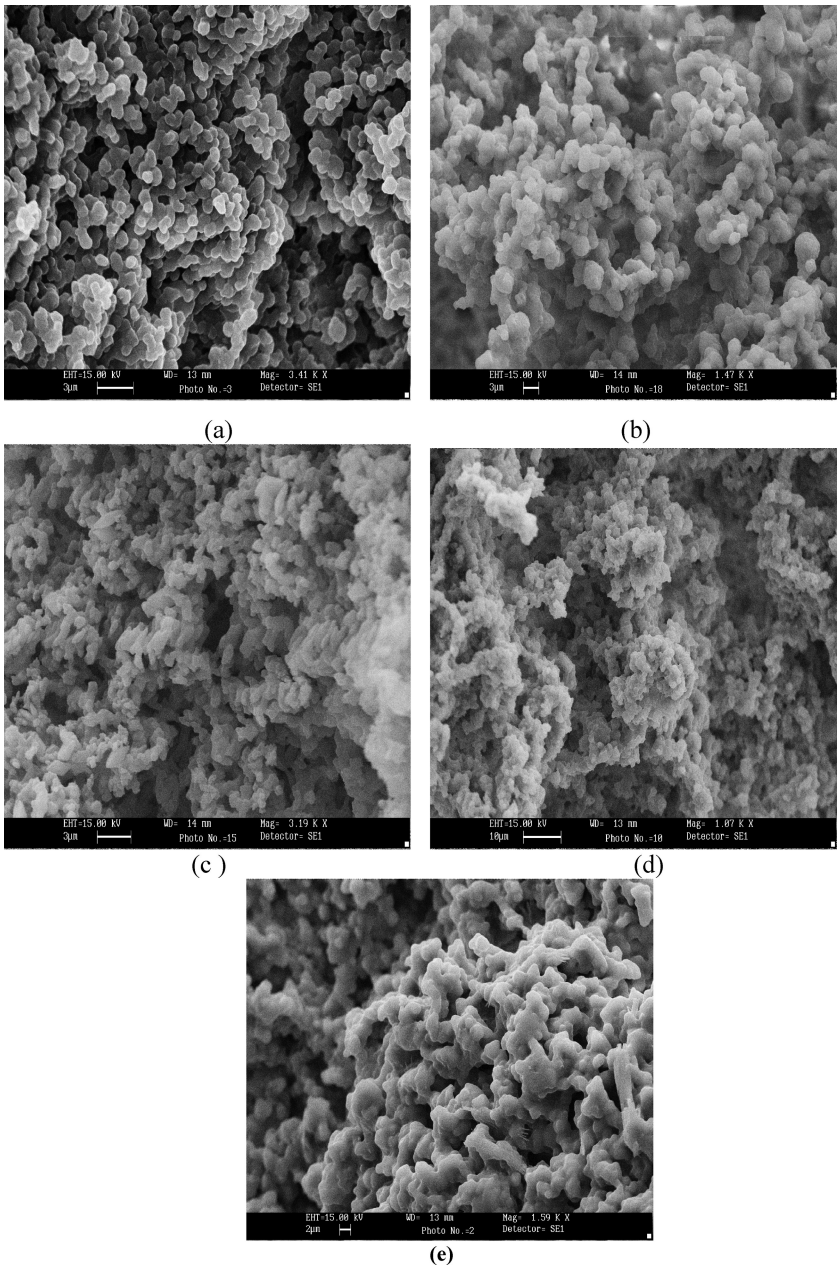

Fig. 9. SEM Micrographs for poly(AM-co-AMPSA) nanogels: (a) CP_0, (b) CP_5, (c) CP_{10}, (d) CP_{15}, and (e) CP_{25}.

group in polymer chain causing shifting of decomposition temperature to lower side.

From DSC measurement, T_g is taken at the midpoint of the transition region. The T_g value of pure PAM nanogel ($T_g = 191.95°C$) is in accordance with the literature ($T_g = 196°C$) (49). It is also observed that by increasing the weight ratio of AMPSA/AM in the copolymer nanogels T_g increases. The increase in T_g values of the copolymer nanogels is due to the presence of sterically bulky propane sulfonic acid group which hinders bond rotation more than smaller groups as well as strong H-bonds.

Figure 9 shows SEM images of poly(AM-co-AMPSA) nanogels with different proportions of AMPSA monomer and pure PAM. Through SEM investigation, it is observed that surface morphology of PAM nanogels is spherical while morphology of poly(AM-co-AMPSA) nanogels changed gradually to elongated cylindrical shape with increasing AMPSA. Micrographs shown in Figure 9(a) for CP_0 nanogels is completely spherical which changes slightly to linked spheres in Figure 9(b) CP_5. However, in Figure 9(c) CP_{10}, the morphology is elongated cylindrical in shape. The maximum dose sulfonic acid monomer in CP_{25} causes enhancement in elongated cylindrical shape with prominent constrictions along the length as shown in Figure 9(e) CP_{25}. The elongated cylindrical shape at high dose of AMPSA content in the nanogels may be due to higher swelling with limited water in the microreactors and constriction of surface arises due to shrinking during drying operations.

4 Conclusions

Nanogel synthesis in the confined environment of microemulsion nanoreactors proves to be very useful for the preparation of functionalized copolymer nanogels of AM and AMPSA. Increase in weight ratio of AMPSA/AM in the copolymer shifts the size of nanogels to a larger particle size with high polydispersity and also causes higher equilibrium swelling. It has also been found that the nanogels possess pH sensitivity. The presence of AMPSA content in the polymer chain shifts the decomposition temperature of the polymer to the higher side.

References

1. Sun, H., Yu, J., Gong, P., Xu, D., Zhang, C. and Yao, S. (2005) *J. Magn. Magn. Mater*., 294, 273.
2. Martinez-Rubio, M.I., Ireland, T.G., Fern, G.R., Silver, J. and Snowden, M.J. (2001) *Langmuir*, 17, 7145.
3. Gong, P., Yu, J., Sun, H., Hong, J., Zhao, S., Xu, D. and Yao, S. (2006) *J. Appl. Polym. Sci.*, 101, 1283.
4. Hong, J., Xu, D., Gong, P., Ma, H., Dong, L. and Yao, S. (2007) *Journ. of Chromatography B*, 850, 499.
5. Nie, L., Jhang, W., Yang, W., Wang, C. and Fu, S. (2005) *Journ. of Mac. Sci., Part A: Pure and Applied Chem*., 42, 623.
6. Chen, G. and Hoffman, A.S. (1995) *Nature*, 35, 795.
7. Chen, G. and Hoffman, A.S. (1995) *Macromol. Rapid Commun*., 16, 175.
8. Yoo, M.K., Sung, Y.K., Cho, C.S. and Lee, Y.M. (1997) *Polymer*, 38, 2759.
9. Tao, L., Vesterinen, E. and Tenhu, H. (1998) *Polymer*, 39, 641.
10. Zhang, J., Xu, S. and Kumacheva, E. (2004) *J. Am. Chem. Soc*., 126, 7908.
11. Shan, J. and Tenhu, H. (2007) *Chem. Commun*., 44, 4580.
12. Xu, S.Q., Zhang, J.G., Paquet, C., Lin, Y.K. and Kumacheva, E. (2003) *Adv. Funct. Mater*., 13, 468.
13. Kim, J.S., Serpe, M.J. and Lyon, L.A. (2005) *Angew. Chem. Int. Ed*., 44, 1333.
14. Zhang, H., Oh, M., Allen, C. and Kumacheva, E. (2004) *Biomacromolecules*, 5, 2461.
15. Soppimath, K.S., Tan, D.C.W. and Yang, Y.Y. (2005) *Adv. Mater*., 17, 318.
16. Vinogradov, S.V. (2006) *Curr. Pharm. Des*., 12, 4703.
17. Kazanskii, K.S. and Dubroskii, S.A. *Advances in Polymer Science*, 104, 97 Springer Berlin/Heidelberg 1992.
18. Buchholz, F.L., Peppas, N.A. (Eds). ACS Symp. Ser. Am Chem Soc, Washington, DC, 573, 1994.
19. Simionescu, C.I. and C. Chelaru, C. (1994) *Polymer Bulletin*, 32, 611.
20. Karlsson, L.E., Jannasch, P. and Wesslen, B. (2002) *Macromol. Chem. and Phys.*, 203, 686.
21. Wu, Y.M., Wang, Y.P., Yu, Y.Q., Xu, J. and Chen, Q.F. (2006) *J. Appl. Polym. Sci*., 102, 2379.
22. Puig, L.J., Sanchez-Diaz, J.C., Villacampa, M., Mendizabal, E., Puig, J.E., Aguiar, A. and Katime, I. (2001) *J. Colloid Interface Sci*., 235, 278.
23. Fernandez, V.V.A., Tepale, N., Sanchez-Diaz, J.C., Mendizabal, E., Puig, J.E. and Soltero, J.F.A. (2006) *Colloid Polym. Sci*., 284, 387.
24. Braun, O., Selb, J. and Candau, F. (2001) *Polymer*, 42, 8499.
25. Antonietti, M., Bremser, W. and Schimdt, M. (1990) *Macromolecules*, 23, 3796.
26. Antonietti, M. (1995) *Macromol. Symp*., 93, 213.
27. Antonietti, M., Pakula, T. and Bremser, W. (1995) Macromolecules, 28, 4227.
28. Topuz, F. and Okay, O. (2009) *React. Funct. Polym.*, 69, 273.
29. McAllister, K., Sazani, P., Adam, M., Cho, M.J., Rubinstein, M., Samulski, R.J. and Desimone, J.D. (2002) *J. Am. Chem. Soc*., 124, 15198.
30. Antonietti, M. (1988) *Angew. Chem. Int. Ed. Engl*., 27, 1743.
31. Travas-Sejdic, J. and Easteal, A.J. (2000) *Polymer*, 41, 7451.
32. Mc Cormick, C.L. and Johnson C.B. (1988) *Macromolecules*, 21, 686.
33. Travas-Sejdic, J. and Easteal, A.J. (2000) *J. Appl. Polym. Sci*., 75, 619.
34. Karg, M., Pastoriza-Santos, I., Rodriguez-Gonzalez, B., Klitzing, R.V., Wellfert, S. and Hellweg, T. (2008) *Langmuir*, 24, 6300.
35. Kazakov, S., Kaholek, M., Kudasheva, D., Teraoka, I., Cowman M.K. and Levon, K. (2003) *Langmuir*, 19, 8086.
36. (a) Pich, A., Tessier, A., Boyko, V., Lu, Y. and Adler, H.-J.P. (2006) *Macromolecules*, 39, 7701; (b) Rubinstein, M., Colby, R.H., Dobrynin, A.V. and Joanny, J.F. (1996) *Macromolecules*, 29, 398.
37. Tong, Z. and Liu, X. (1994) *Macromolecules*, 27, 844.
38. Liu, X., Tong, Z. and Hu, O. (1995) *Macromolecules*, 28, 3813.
39. Zhang, C. and Easteal, A.J. (2007) *J. Appl. Polym. Sci*., 104, 1723.
40. Lu, X. and Mi, Y. (2005) *Macromolecules*, 38, 839.
41. Rosa, F., Bordado, J. and Casquilho, M. (2003) *J. Appl. Polym. Sci*., 87, 192.

42. Sabhapondit, A., Borthakur, A. and Haque, I. (2003) *J. Appl. Polym. Sci*., 87, 1869.
43. Daubresse, C., Grandfils, Ch., Jerome, R. and Tessyie, Ph. (1996) *Colloid Polym. Sci.*, 274, 482.
44. Aggour, Y.A. (1994) *Polym. Degrad. Stab*., 44, 71.
45. Bhardwaj, P., Singh, S., Singh, V., Aggarwal, S. and Mandal, U.K. (2008) *Int. J. Polym. Mater*., 57, 404.
46. Caulfield, M.J., Qiao, G.G. and Solomon, D. H. (2002) *Chem. Rev*., 102, 3067.
47. Devrim, Y.G., Rzaev, Z. M. O. and Piskin, E. (2006) *Macromol. Chem. Phys*., 207, 111.
48. Zhang, C. and Easteal, A.J. (2003) *J. Appl. Polym. Sci*., 89, 1322.
49. Janigova, I., Csomorova, K., Stillhammerova, M. and Barton, J. (1994) *J. Macromol. Chem. Phys*., 195, 3609.